ISSN 0915-633X

NATIONAL INSTITUTE FOR FUSION SCIENCE

V-shaped dc Potential Structure Caused by Current-driven Electrostatic Ion-cyclotron Instability

S. Ishiguro T. Sato, H. Takamaru and
The Complexity Simulation Group

(Received - Mar. 27, 1997)

NIFS-493 May 1997

RESEARCH REPORT
NIFS Series

NAGOYA, JAPAN

V-shaped dc potential structure caused by current-driven electrostatic ion-cyclotron instability

Seiji Ishiguro

Department of Electronic Engineering, Tohoku University,

Sendai 980-77, Japan

Tetsuya Sato, Hisanori Takamaru, and The Complexity Simulation Group*

Theory and Computer Simulation Center, National Institute for Fusion Science,

Nagoya 464-01, Japan

Abstract

It is first demonstrated that a V-shaped dc potential structure is created by a current-driven electrostatic ion-cyclotron instability by means of an open two-dimensional particle simulation model. A positive dc potential difference along magnetic field lines is generated by anomalous resistivity caused by the ion-cyclotron instability. In the direction across the magnetic field lines dc potential rises from the high current region to the low current region.

Keywords: ion cyclotron wave, wave front pattern, instability, current, particle simulation, V-shaped potential structure, parallel electric field, aurora.

---

*K. Watanabe, R. Horiuchi, T. Hayashi, Y. Todo, T.-H. Watanabe, and A. Kageyama

Formation of electric field along magnetic field lines is as yet a puzzling and challenging problem for generating accelerated charged particles in a space plasma [1]. In particular, many space observations support that auroral electrons are accelerated by a parallel electric field above the ionosphere [2–4]. Current-driven kinetic instabilities such as ion acoustic and electrostatic ion-cyclotron instabilities have been paid much attentions as such candidates. It is well known that double layers are created by an ion acoustic instability for a relatively high electron stream [5–7]. On the other hand, analysis says that electrostatic ion-cyclotron waves become unstable for a smaller electron stream in an isothermal plasma [8,9] and in fact that are frequently observed by satellite observations. Furthermore, it is reported that a V-shaped potential structure and electrostatic ion cyclotron wave are simultaneously present above the auroral ionosphere [10]. In the past Swift [11] proposed an auroral electron acceleration model based on a oblique electrostatic shock caused by a current-driven electrostatic ion-cyclotron instability. However, the steady state theory can not answer the question how shock is created. Although many laboratory experiments [12,13] and numerical simulations [14,15] concerned with a V-shaped potential structure or an ion-cyclotron instability have been performed, no one succeeded in demonstrating that current-driven electrostatic ion-cyclotron instability creates a V-shaped potential structure.

With these situations in mind, we investigate development of a current-driven electrostatic ion-cyclotron instability and resulting dc potential structure with special attention on two dimensional structure by means of a sophisticated particle simulation model.

In our previous particle simulation [16], we observed a clear wave front pattern accompanied by the ion-cyclotron instability. In that simulation we used a periodic boundary condition for both particles and fields, namely, particles going out one boundary periodically enter the system from the other boundary. Because of no supply of fresh streaming particles the growth of the wave amplitude saturates at a low level and no observable dc potential structure is created. In the auroral field line region, however, the origin of the streaming electrons along the field lines is supposed to be in the plasma sheet. This means that the field-aligned electron stream, or, field-aligned current, is continuously supplied by fresh magnetospheric electrons. Therefore, the periodic boundary condition is not an appropriate for both particles and fields. In order to remove the periodic boundary condition and to make a more realistic situation, we have developed a two-and-half dimensional open boundary simulation code adopting the method developed by Takamaru *et al.* [17,7] for a one dimensional simulation.

We have developed a two-and-half dimensional electrostatic open boundary particle simulation model where fresh particles are injected from the boundaries at each time step avoiding unphysical accumulation of charged particles in front of the boundaries. A schematic view of simulation model is presented in Fig. 1. Uniform external magnetic field is pointing into the positive x direction. A periodic boundary condition is applied in the y direction, whereas the left and right boundaries are open. The system is divided in segments in the y direction where each segment is assumed to be connected to an external constant current generator, respectively. The number of particles injected from the open boundaries in the x direction are specified in such a way that the electric current is kept constant at the boundaries of each segment at each time step. The velocity distribution of injected particles are specified so as to be consistent with the initial particle velocity distribution. This procedure is applied for electrons. For ions, however, the reflection boundary condition is applied. This is because we assume a shifted Maxwellian electron and a non-shifted Maxwellian ion.

The ion motion is followed in (v_x, v_y, v_z) space to track the ion cyclotron motion, whereas we adopt the drift kinetic approximation for electrons and the electron motion is traced only along the magnetic field lines. This is because the electric field has only x and y components, so particle $E \times B$ drift motion is pointing into the z direction which is no meaning in our configuration.

Simulation parameters used in this paper are as follows: The system sizes are $L_x = 512\lambda_{De}$ and $L_y = 128\lambda_{De}$ and grid number is 512×128, where λ_{De} is the Debye length. The system is assumed to be divided into 16 segments in the y direction, and thus the width of each segment is $8\lambda_{De}$. The number of ions and electrons are 67108864, respectively, and thus, 1024 particles per unit grid cell are used. The ion to electron mass ratio is 400 and the temperature ratio is 1/2. The electron cyclotron frequency $\omega_{ce} = 5\omega_{pe}$ and the ion cyclotron frequency is $\omega_{ci} = 0.0125\omega_{pe}$, where ω_{pe} is the electron plasma frequency. The electron velocity distribution is a shifted Maxwellian with drifting into the x direction, and the drift velocity is given by $v_{de}(y) = [0.6 - 0.2\cos(2\pi y/L_y)]v_{te}$. Here, $v_{te}(= (T_e/m_e)^{1/2})$ is the electron thermal velocity, T_e and m_e are the electron temperature (Energy unit) and the electron mass. The time step width $\omega_{pe}\Delta t$ is 0.2.

First of all, we show the growth of ion-cyclotron instability. Figure 2 shows time evolution of the magnitude of the ion density fluctuation (a) and the frequency spectrum (b) for the mode with $k_\perp\rho_i = 0.825$ and $k_\parallel\rho_i = 0.103$. This is the typical unstable mode for the electrostatic ion cyclotron wave for our choice of simulation parameters. It should be noted that the amplitude of the ion density fluctuation continuously increases for a long time, whereas in the previous simulation [16] with the periodic model (the same parameters) the growth saturates at a lower level around $\omega_{pe}t \simeq 4000$. This indicates that the injection of fresh drifting electrons from the boundaries much more activates the instability development. The peak of the frequency is around $\omega \simeq \pm 1.4\omega_{ci}$, indicating that the mode corresponds to the ion cyclotron wave.

An exponential growth is not clearly observed in the initial phase. This is because the ion cyclotron wave is unstable only in the high-stream region and the system is open, and thus the excited wave goes away from the unstable region.

We shall show a long time evolution of the ion density profile, which is averaged over the three times of the electron plasma period $3\times 2\pi/\omega_{pe}$ in Fig. 3. At $\omega_{pe}t = 500$, one can see only small scale smeared fluctuations in the whole system. It is important to note that no sheath-like or any artificial noises appear near the upstream and downstream boundaries, although fresh electrons are injected from the boundaries. A V-shaped stripe pattern appearing at $\omega_{pe}t = 1000$ in the region with $x/\lambda_{De} \gtrsim 150$ and $30 \lesssim y/\lambda_{De} \lesssim 100$ grows with time and becomes clear at $\omega_{pe}t = 3000$. At $\omega_{pe}t = 6000$. V-shaped wave front pattern is well developed for $x/\lambda_{De} \gtrsim 200$ The angle between the wave front and the magnetic filed lines is ± 7 degrees, namely, $|k_y/k_x| \simeq 0.12$. The amplitude is larger in the downstream region than in the upstream region.

Figure 4 shows the gray scale contour plots of the potential profile at $\omega_{pe}t = 6000$. A clear V-shaped wave front pattern is seen around $x/\lambda_{De} \sim 380$ and $y/\lambda_{De} \sim 70$. The angle between the equi-potential lines and magnetic field lines are ± 7 degrees, which is the same as for the ion density profile.

In order to see the time variation of the ion density profile in a short time interval, we plot the ion density profiles at 5900, 6000, and 6100 in Fig. 5. Careful examination of three profiles concludes that that the wave fronts propagate from the high stream region (around $y/\lambda_{De} \simeq 64$) to the low stream region (around $y/\lambda_{De} \simeq 0$ and 128) with angle ± 83 degrees with respect to the magnetic field lines. The wave length is roughly $20\lambda_{De}$ and the speed of propagation is roughly $0.06v_{te}$.

Finally, we shall see the dc potential profile. Figure 6 shows that the gray scale contour plot of potential profile together with the potential profiles along the magnetic field lines at $y/\lambda_{De} = 64$ and across the magnetic field lines at $x/\lambda_{De} = 320$, 370, and 430. These are averaged over the period of oscillation of the electrostatic ion cyclotron wave. The potential gradually rises up from $x/\lambda_{De} \simeq 300$ to the downstream boundary along the magnetic field lines. The total potential difference reaches about $e\Delta\phi/T_e \simeq 0.02$.

Since the electric current is kept constant in this simulation, the anomalous resistivity can be calculated from the relation $\eta = eE/n_0 e^2 v_{de} = e(\Delta\phi/l)\phi/n_0 e^2 v_{de}$. Using the above results with $e\Delta\phi/T_e \simeq 0.02$, $l = 200\lambda_{De}$, $v_{de} = 0.8v_{te}$ at $\omega_{pe}t = 7000$, one can get $\eta/\eta_0 \simeq 1.2 \times 10^{-4}$, where $\eta_0 = 4\pi/\omega_{pe}$. In the y direction the potential profile has a small well. Though not so clearly structured, one can certainly recognized a V-shaped dc potential structure in the downstream region.

We have developed a two-and-half dimensional electrostatic open boundary particle simulation code where fresh particles are supplied from the boundaries with a specified velocity distribution without generating any artificial potential irregularities. Using this code, we have studied the wave front pattern and the formation of a dc potential structure along the magnetic field caused by a current-driven electrostatic ion-cyclotron instability. The amplitude of the ion cyclotron wave grows continuously beyond the level of saturation of the previous periodic particle simulation. A V-shaped wave front pattern arises which manifests as an interface pattern of the waves propagating from the high stream region to the low stream region.

The ion cyclotron wave is excited in the upstream region and develops as it propagates from the upstream region to the downstream region. It grows significantly when it crosses the high electron-stream region, thus, it has a large amplitude when it propagates from the high electron-stream region to the low region. Hence a V-shaped wave front pattern arises.

It is interestingly to observed that a V-shaped dc potential structure is created by the electrostatic ion-cyclotron instability. The dc potential gradually grows from the center of the system to the downstream region. This dc potential difference along the magnetic filed lines is supposed to be created by the anomalous resistivity caused by the ion cyclotron waves. The potential difference is larger in the high electron-stream region than in the low electron-stream region. The anomalous resistivity estimated from the created potential difference is much larger than the value obtained from the initial value periodic simulation.

We have observed a potential well across the magnetic field lines. This may be caused by the ion transport from the high stream region to the low stream region or the difference of ion perpendicular heating across the magnetic field lines.

The growth of the amplitude of ion cyclotron wave stops neither temporally nor spatially within the limit of the present simulation run. Thus it is likely that a larger potential difference may be created for a larger and longer simulation system. If we assume that the potential difference is proportional to the system length, one can get several kV potential differences for $T_e = 1\text{eV}$, $n_e = 10^2\text{cm}^{-2}$, and several thousand kilometers anomalous resistivity region [18], which is consistent with the auroral electron acceleration.

In conclusion we have succeeded in the first time a two dimensional particle simulation which demonstrates that the V-shaped dc potential structure is created by the current-driven electrostatic ion-cyclotron instability.

One of the authors (S. I.) would like to thank Professor Noriyoshi Sato for his encouragement. The computations were performed at the Advanced Computing System for Complexity Simulation at the National Institute for Fusion Science.

REFERENCES

[1] C.-G. Fälthammar, Rev. Geophys. Space Phys. **15**, 457 (1977).

[2] L. A. Frank and K. L. Ackerson, J. Geophys. Res. **76**, 3612 (1971).

[3] D. Evans, J. Geophys. Res. **74**, 2853 (1974).

[4] R. L. Arnoldy, P. B. Lewis, and P. O. Issacson, J. Geophys. Res. **79**, 4208 (1974).

[5] T. Sato and H. Okuda, Phys. Rev. Lett. **44**, 740 (1980); J. Geophys. Res. **86**, 3357 (1981).

[6] C. Barnes, M. K. Hudson, and W. Lotko, Phys. Fluids **28**, 1055 (1985).

[7] T. Sato, H. Takamaru, and the Complexity Simulation Group, Phys. Plasmas **2**, 3609 (1995).

[8] W. E. Drummond and M. N. Rosenbluth, Phys. Fluids **5**, 1507 (1962).

[9] J. M. Kindel and C. F. Kennel, J. Geophys. Res. **76**, 3055 (1971).

[10] F. S. Mozer, C. W. Carlson, M. K. Carlson, M. K. Hudson, R. B. Torbert, B. Parady, and J. Yatteau, Phys. Rev. Lett. **7**, 292 (1977).

[11] D. W. Swift, J. Geophys. Res. **84**, 6427 (1979).

[12] M. J. Alport, S. L. Cartier, and R. L. Merlino, J. Geophys. Res. **91**, 1599 (1986).

[13] N. Sato, M. Nakamura, and R. Hatakeyama, Phys. Rev. Lett. **57**, 1227 (1986).

[14] J. S. Wagner, T. Tajima, J. R. Kan, J. N. Leboeuf, S. -I. Akasofu, and J. M. Dawson, Phys. Rev. Lett. **45**, 803 (1980).

[15] H. Okuda, C. Z. Chen, and W. W. Lee, Phys. Fluids **24**, 1060 (1981).

[16] S. Ishiguro, T. Sato, H. Takamaru, K. Watanabe and the Complexity Simulation Group, "Formation of wave-front pattern accompanied by current-driven electrostatic

ion-cyclotron instabilities," submitted to Phys. Plasmas (1997).

[17] H. Takamaru, T. Sato, R. Horiuchi, K. Watanabe, and the Complexity Simulation Group, "A self-consistent open boundary model for particle simulation in plasmas," submitted to J. Comput. Phys. (1995).

[18] M. K. Hudson, R. L. Lysak, and F. S. Mozer, Geophys. Res. Lett. **5**, 143 (1978).

Figure Captions

Fig. 1. Open boundary simulation system connected to constant current generators.

Fig. 2. Time history of ion density fluctuation (a) and frequency spectrum (b) with $k_{\|}\rho_i = 0.103$ and $k_{\perp}\rho_i = 0.825$.

Fig. 3. Gray scale plots of the ion density fluctuation at $\omega_{pe}t = 500$, 1000, 3000, and 6000.

Fig. 4. Gray scale contour plot of the potential profile at $\omega_{pe}t = 6000$.

Fig. 5. Gray scale plots of the ion density fluctuation at $\omega_{pe}t = 5900$, 6000, and 6100.

Fig. 6. Gray scale contour plot of the dc potential profile together with the x direction profile at $y/\lambda_{De} = 64$ and the y direction profiles at $x/\lambda_{De} = 320$, 370, and 430 at $\omega_{pe}t = 7000$.

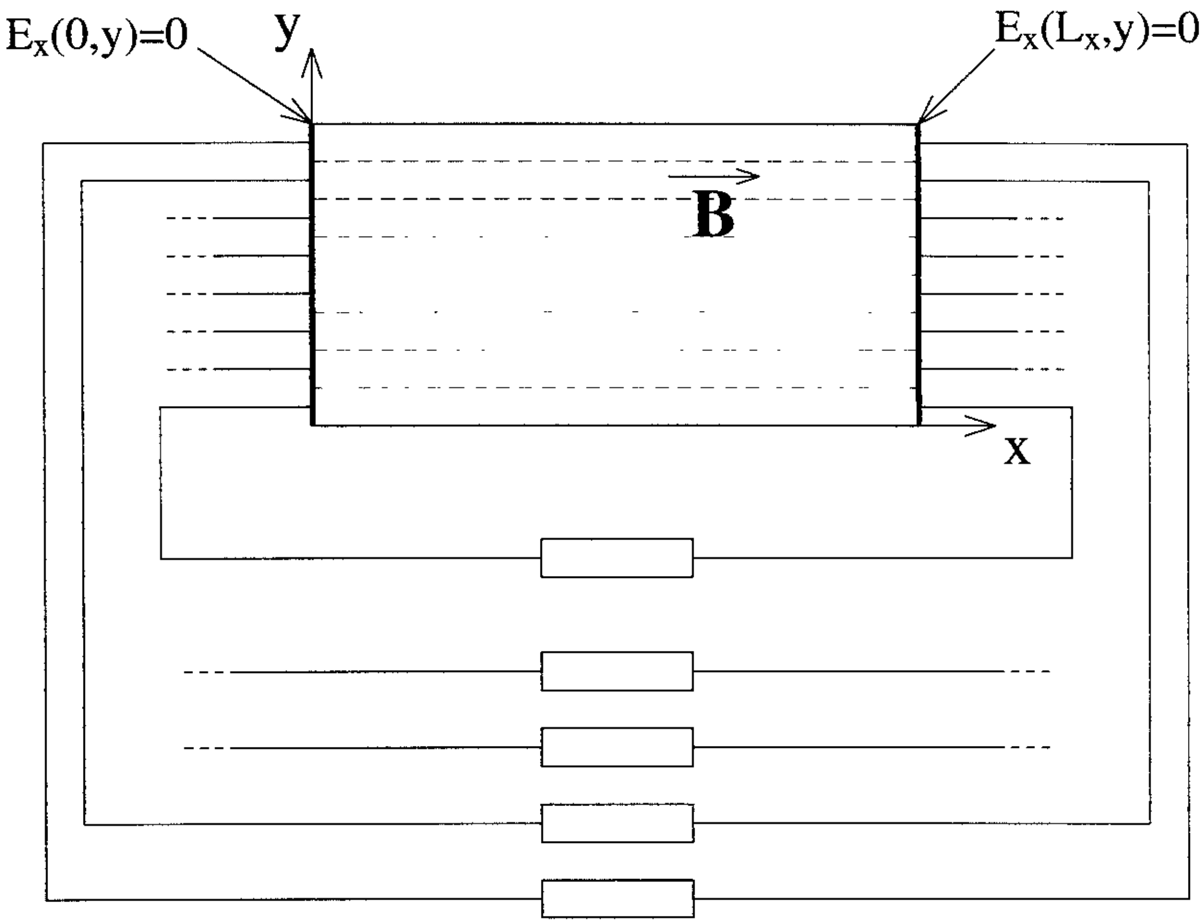

Constant Current Generators

Fig. 1

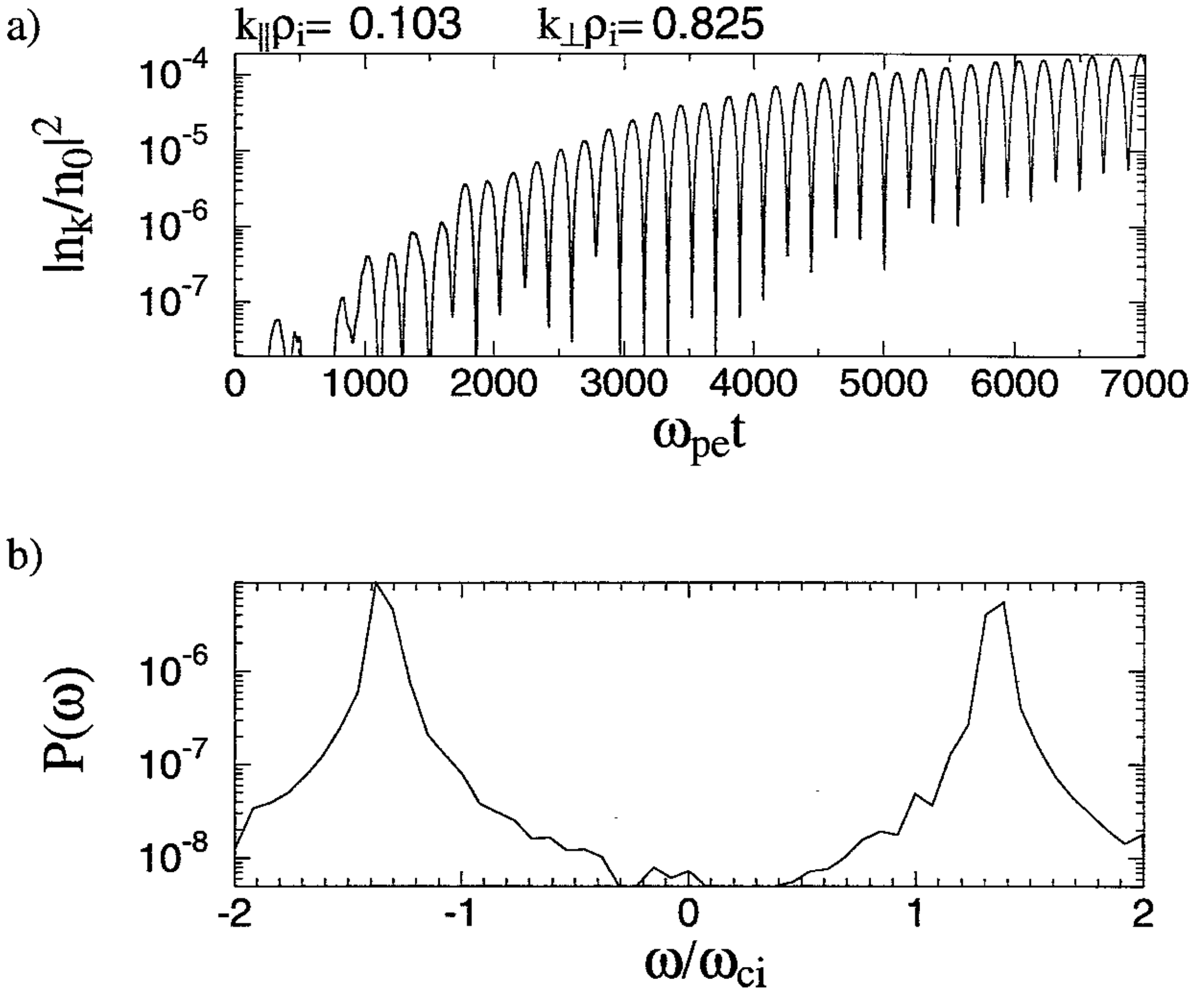

a)
k∥ρi= 0.103 k⊥ρi= 0.825
|nk/n0|^2
10^-4
10^-5
10^-6
10^-7
0 1000 2000 3000 4000 5000 6000 7000
ωpet
b)
P(ω)
10^-6
10^-7
10^-8
-2 -1 0 1 2
ω/ωci

Fig. 2

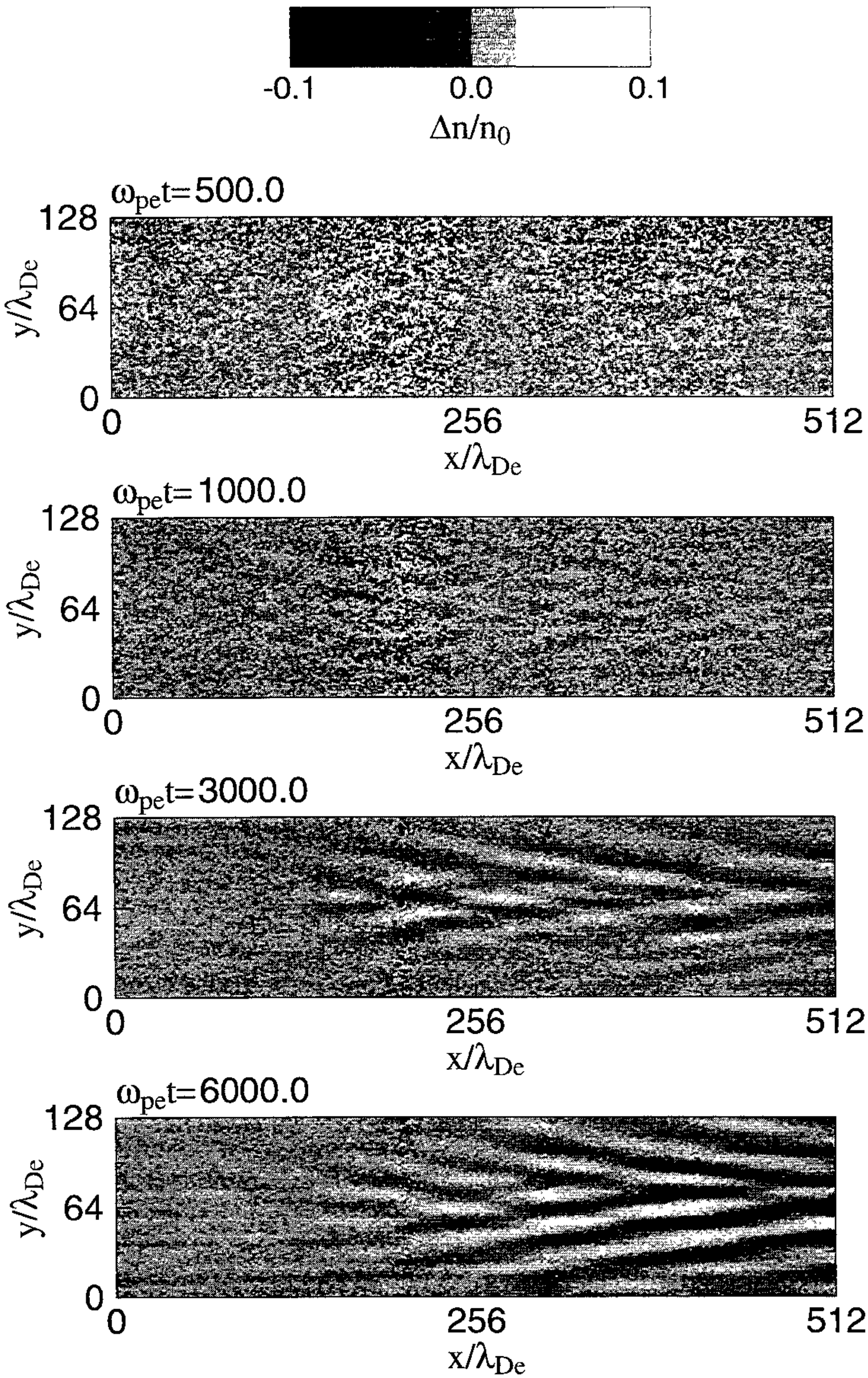
-0.1
0.0
0.1
Δn/n0
ωpet=500.0
ωpet=1000.0
ωpet=3000.0
ωpet=6000.0
128
64
0
y/λDe
0
256
512
x/λDe

Fig. 3

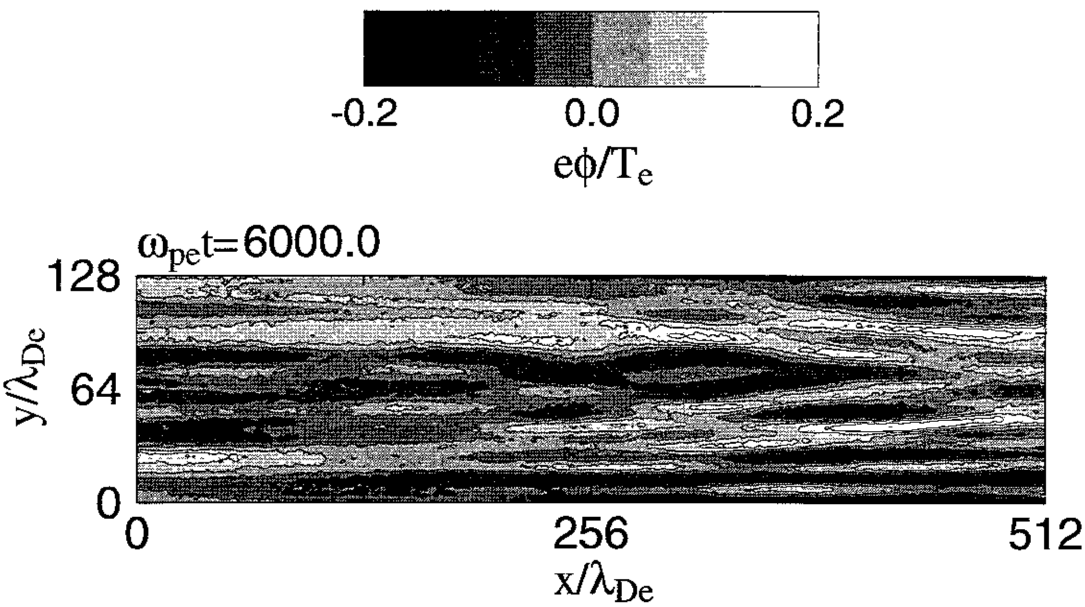

Fig. 4

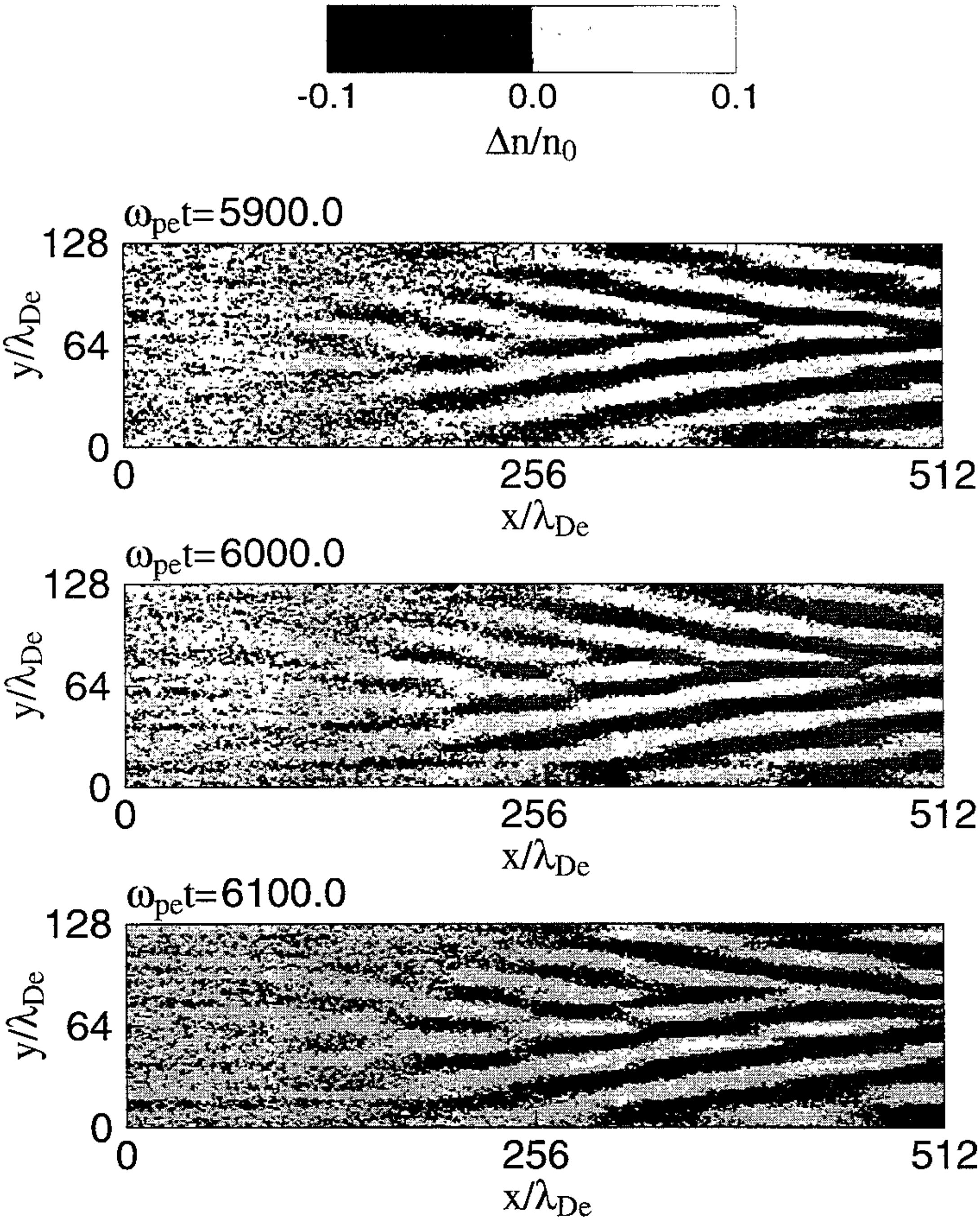

-0.1
0.0
0.1
Δn/n0
ωpet=5900.0
128
y/λDe
64
0
0
256
512
x/λDe
ωpet=6000.0
128
y/λDe
64
0
0
256
512
x/λDe
ωpet=6100.0
128
y/λDe
64
0
0
256
512
x/λDe

Fig. 5

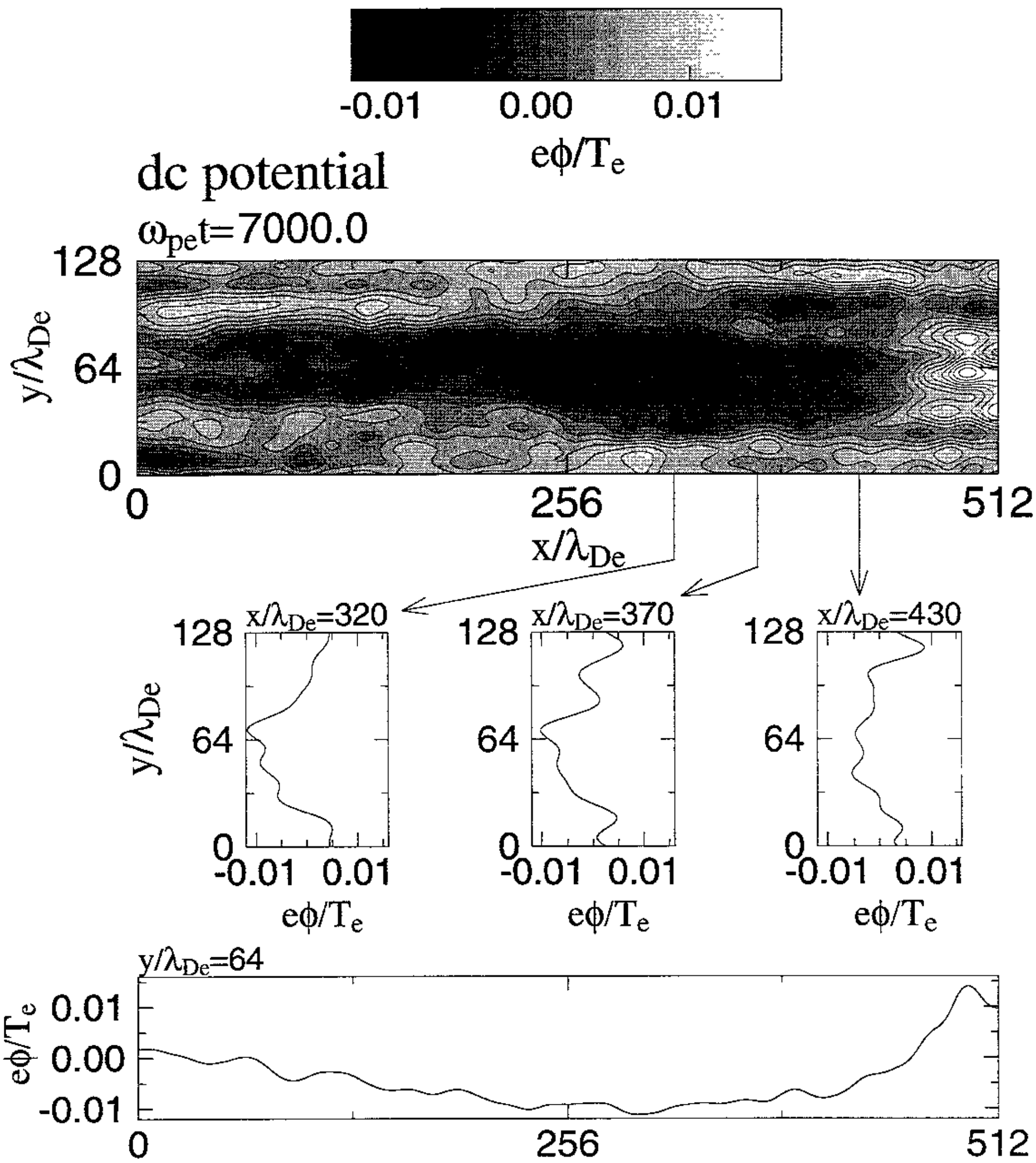

-0.01
0.00
0.01
eφ/Te
dc potential
ωpet=7000.0
128
64
0
y/λDe
0
256
512
x/λDe
x/λDe=320
x/λDe=370
x/λDe=430
-0.01 0.01
eφ/Te
y/λDe=64

Fig. 6

Recent Issues of NIFS Series

NIFS-448 M. Ozaki, T. Sato and the Complexity Simulation Group,
Interactions of Convecting Magnetic Loops and Arcades; Sep. 1996

NIFS-449 T. Aoki,
Interpolated Differential Operator (IDO) Scheme for Solving Partial Differential Equations; Sep. 1996

NIFS-450 D. Biskamp and T. Sato,
Partial Reconnection in the Sawtooth Collapse; Sep. 1996

NIFS-451 J. Li, X. Gong, L. Luo, F.X. Yin, N. Noda, B. Wan, W. Xu, X. Gao, F. Yin, J.G. Jiang, Z. Wu., J.Y. Zhao, M. Wu, S. Liu and Y. Han,
Effects of High Z Probe on Plasma Behavior in HT-6M Tokamak; Sep. 1996

NIFS-452 N. Nakajima, K. Ichiguchi, M. Okamoto and R.L. Dewar,
Ballooning Modes in Heliotrons/Torsatrons; Sep. 1996 (IAEA-CN-64/D3-6)

NIFS-453 A. Iiyoshi,
Overview of Helical Systems; Sep. 1996 (IAEA-CN-64/O1-7)

NIFS-454 S. Saito, Y. Nomura, K. Hirose and Y.H. Ichikawa,
Separatrix Reconnection and Periodic Orbit Annihilation in the Harper Map; Oct. 1996

NIFS-455 K. Ichiguchi, N. Nakajima and M. Okamoto,
Topics on MHD Equilibrium and Stability in Heliotron / Torsatron; Oct. 1996

NIFS-456 G. Kawahara, S. Kida, M. Tanaka and S. Yanase,
Wrap, Tilt and Stretch of Vorticity Lines around a Strong Straight Vortex Tube in a Simple Shear Flow; Oct. 1996

NIFS-457 K. Itoh, S.- I. Itoh, A. Fukuyama and M. Yagi,
Turbulent Transport and Structural Transition in Confined Plasmas; Oct. 1996

NIFS-458 A. Kageyama and T. Sato,
Generation Mechanism of a Dipole Field by a Magnetohydrodynamic Dynamo; Oct. 1996

NIFS-459 K. Araki, J. Mizushima and S. Yanase,
The Non-axisymmetric Instability of the Wide-Gap Spherical Couette Flow; Oct. 1996

NIFS-460 Y. Hamada, A. Fujisawa, H. Iguchi, A. Nishizawa and Y. Kawasumi,
A Tandem Parallel Plate Analyzer; Nov. 1996

NIFS-461 Y. Hamada, A. Nishizawa, Y. Kawasumi, A. Fujisawa, K. Narihara, K. Ida, A. Ejiri, S. Ohdachi, K. Kawahata, K. Toi, K. Sato, T. Seki, H. Iguchi, K. Adachi, S. Hidekuma, S.Hirokura. K. Iwasaki, T. Ido, M. Kojima, J. Koong, R. Kumazawa, H. Kuramoto, T. Minami, I. Nomura, H. Sakakita, M. Sasao, K.N. Sato, T. Tsuzuki, J. Xu, I. Yamada and T. Watari,
Density Fluctuation in JIPP T-IIU Tokamak Plasmas Measured by a Heavy Ion Beam Probe; Nov. 1996

NIFS-462 N. Katsuragawa, H. Hojo and A. Mase,
Simulation Study on Cross Polarization Scattering of Ultrashort-Pulse Electromagnetic Waves; Nov. 1996

NIFS-463 V. Voitsenya, V. Konovalov, O. Motojima, K. Narihara, M. Becker and B. Schunke,
Evaluations of Different Metals for Manufacturing Mirrors of Thomson Scattering System for the LHD Divertor Plasma; Nov. 1996

NIFS-464 M. Pereyaslavets, M. Sato, T. Shimozuma, Y. Takita, H. Idei, S. Kubo, K. Ohkubo and K. Hayashi,
Development and Simulation of RF Components for High Power Millimeter Wave Gyrotrons; Nov. 1996

NIFS-465 V.S. Voitsenya, S. Masuzaki, O. Motojima, N. Noda and N. Ohyabu.
On the Use of CX Atom Analyzer for Study Characteristics of Ion Component in a LHD Divertor Plasma; Dec. 1996

NIFS-466 H. Miura and S. Kida,
Identification of Tubular Vortices in Complex Flows; Dec. 1996

NIFS-467 Y. Takeiri, Y. Oka, M. Osakabe, K. Tsumori, O. Kaneko, T. Takanashi, E. Asano, T. Kawamoto, R. Akiyama and T. Kuroda,
Suppression of Accelerated Electrons in a High-current Large Negative Ion Source; Dec. 1996

NIFS-468 A. Sagara, Y. Hasegawa, K. Tsuzuki, N. Inoue, H. Suzuki, T. Morisaki, N. Noda, O. Motojima, S. Okamura, K. Matsuoka, R. Akiyama, K. Ida, H. Idei, K. Iwasaki, S. Kubo, T. Minami, S. Morita, K. Narihara, T. Ozaki, K. Sato, C. Takahashi, K. Tanaka, K. Toi and I. Yamada,
Real Time Boronization Experiments in CHS and Scaling for LHD; Dec. 1996

NIFS-469 V.L. Vdovin, T.Watari and A. Fukuyama,
3D Maxwell-Vlasov Boundary Value Problem Solution in Stellarator Geometry in Ion Cyclotron Frequency Range (final report); Dec. 1996

NIFS-470 N. Nakajima, M. Yokoyama, M. Okamoto and J. Nührenberg,
Optimization of M=2 Stellarator; Dec. 1996

NIFS-471 A. Fujisawa, H. Iguchi, S. Lee and Y. Hamada,
Effects of Horizontal Injection Angle Displacements on Energy Measurements with Parallel Plate Energy Analyzer; Dec. 1996

NIFS-472 R. Kanno, N. Nakajima, H. Sugama, M. Okamoto and Y. Ogawa,
Effects of Finite-β and Radial Electric Fields on Neoclassical Transport in the Large Helical Device; Jan. 1997

NIFS-473 S. Murakami, N. Nakajima, U. Gasparino and M. Okamoto,
Simulation Study of Radial Electric Field in CHS and LHD; Jan. 1997

NIFS-474 K. Ohkubo, S. Kubo, H. Idei, M. Sato, T. Shimozuma and Y. Takita,
Coupling of Tilting Gaussian Beam with Hybrid Mode in the Corrugated Waveguide; Jan. 1997

NIFS-475 A. Fujisawa, H. Iguchi, S. Lee and Y. Hamada,
Consideration of Fluctuation in Secondary Beam Intensity of Heavy Ion Beam Prove Measurements; Jan. 1997

NIFS-476 Y. Takeiri, M. Osakabe, Y. Oka, K. Tsumori, O. Kaneko. T. Takanashi, E. Asano, T. Kawamoto, R. Akiyama and T. Kuroda,
Long-pulse Operation of a Cesium-Seeded High-Current Large Negative Ion Source; Jan. 1997

NIFS-477 H. Kuramoto, K. Toi, N. Haraki, K. Sato, J. Xu, A. Ejiri, K. Narihara, T. Seki, S. Ohdachi, K. Adatı, R. Akiyama, Y. Hamada, S. Hirokura, K. Kawahata and M. Kojima,
Study of Toroidal Current Penetration during Current Ramp in JIPP T-IIU with Fast Response Zeeman Polarimeter; Jan., 1997

NIFS-478 H. Sugama and W. Horton,
Neoclassical Electron and Ion Transport in Toroidally Rotating Plasmas; Jan. 1997

NIFS-479 V.L. Vdovin and I.V. Kamenskij,
3D Electromagnetic Theory of ICRF Multi Port Multi Loop Antenna; Jan. 1997

NIFS-480 W.X. Wang, M. Okamoto, N. Nakajima, S Murakami and N. Ohyabu,
Cooling Effect of Secondary Electrons in the High Temperature Divertor Operation; Feb. 1997

NIFS-481 K. Itoh, S.-I. Itoh, H. Soltwisch and H.R. Koslowski,
Generation of Toroidal Current Sheet at Sawtooth Crash; Feb. 1997

NIFS-482 K. Ichiguchi,
Collisionality Dependence of Mercier Stability in LHD Equilibria with Bootstrap Currents; Feb. 1997

NIFS-483 S. Fujiwara and T. Sato,
Molecular Dynamics Simulations of Structural Formation of a Single Polymer Chain: Bond-orientational Order and Conformational Defects; Feb. 1997

NIFS-484 T. Ohkawa,
Reduction of Turbulence by Sheared Toroidal Flow on a Flux Surface; Feb. 1997

NIFS-485 K. Narihara, K. Toi, Y. Hamada, K. Yamauchi, K. Adachi, I. Yamada, K. N. Sato, K. Kawahata, A. Nishizawa, S. Ohdachi, K. Sato, T. Seki, T. Watari, J. Xu, A. Ejiri, S. Hirokura, K. Ida, Y. Kawasumi, M. Kojima, H. Sakakita, T. Ido, K. Kitachi. J. Koog and H. Kuramoto,
Observation of Dusts by Laser Scattering Method in theJIPPT-IIU Tokamak Mar. 1997

NIFS-486 S. Bazdenkov, T. Sato and The Complexity Simulation Group,
Topological Transformations in Isolated Straight Magnetic Flux Tube; Mar. 1997

NIFS-487 M. Okamoto,
Configuration Studies of LHD Plasmas; Mar. 1997

NIFS-488 A. Fujisawa, H. Iguchi, H. Sanuki, K. Itoh, S. Lee, Y. Hamada, S. Kubo. H. Idei, R. Akiyama, K. Tanaka, T. Minami, K. Ida, S. Nishimura, S. Morita, M. Kojima, S. Hidekuma, S.-I. Itoh, C. Takahashi, N. Inoue, H. Suzuki, S. Okamura and K. Matsuoka.
Dynamic Behavior of Potential in the Plasma Core of the CHS Heliotron/Torsatron; Apr. 1997

NIFS-489 T. Ohkawa,
Pfirsch - Schlüter Diffusion with Anisotropic and Nonuniform Superthermal Ion Pressure; Apr. 1997

NIFS-490 S. Ishiguro and The Complexity Simulation Group,
Formation of Wave-front Pattern Accompanied by Current-driven Electrostatic Ion-cyclotron Instabilities; Apr. 1997

NIFS-491 A. Ejiri, K. Shinohara and K. Kawahata,
An Algorithm to Remove Fringe Jumps and its Application to Microwave Reflectometry; Apr. 1997

NIFS-492 K. Ichiguchi, N. Nakajima, M. Okamoto,
Bootstrap Current in the Large Helical Device with Unbalanced Helical Coil Currents; Apr. 1997

NIFS-493 S. Ishiguro, T. Sato, H. Takamaru and The Complexity Simulation Group,
V-shaped dc Potential Structure Caused by Current-driven Electrostatic Ion-cyclotron Instability; May 1997